J. Fluid Mech. (1989), *vol.* 199, *pp.* 237–255
Printed in Great Britain

Semi-preserving development of a slightly heated free swirling jet

By J. W. ELSNER AND L. KURZAK
Thermal Machinery Institute, Technical University of Częstochowa, Deglera 35, 42-200 Częstochowa, Poland

(Received 10 August 1987 and in revised form 3 March 1988)

The paper formulates the concept of a semi-preserving developing of a free non-isothermal swirling jet. On the basis of experimental data it may be estimated that the semi-preserving conditions are established at the distance $x-x_0 \approx (15\text{–}20)\,D$. Also, it has been pointed out that self-preservation, which requires the turbulence structure to be similar during decay, may be considered as an asymptotic state of the semi-preserving development achieved in practice at a distance where $\overline{u_r u_\varphi}/\overline{u_x u_r} \ll 1.0$.

1. Introduction

For many years free swirling jets have been thoroughly investigated on account of their wide application in industrial practice as well as because they constitute a type of flow which is interesting from the theoretical point of view as it combines the characteristics of a rotating turbulent motion and non-isotropic free turbulence phenomena. The additional circumferential motion produces not only a virtual change of the mean flow pattern but also significantly modifies the turbulence structure by intensifying the processes of the turbulent transport of mass, momentum and heat, especially in the near flow region.

So far, research on swirling jets has mainly been undertaken using experimental methods. Regarding isothermal flows, one should mention here the works by, for example, Rose (1962), Chigier & Chervinsky (1967), Pratte & Keffer (1972), Elsner & Drobniak (1983), Grandmaison & Becker (1982) and others.

The evolution of non-isothermal swirling jets, with special attention paid to the development of the temperature field and the problem of turbulent heat diffusion has, in turn, been studied by Curtet & Darigol (1978), Komori & Ueda (1985) and Elsner & Kurzak (1987).

In any theoretical description of turbulent free flows it is very convenient to make use of the self-preservation hypothesis. This is based on the assumption that the transverse distributions of mean and turbulent velocity components may be made identical when presented in reduced forms with the aid of one velocity scale (U^*), and one lengthscale (l^*), as functions of the stream coordinate alone. It goes without saying that such an assumption results in considerable simplification of the flow description, as it reduces the number of independent variables and transforms the governing partial differential equations into a set of ordinary differential equations.

The problem of the self-preserving development of free, unswirled axisymmetric jets has been studied, *inter alia*, by Wygnanski & Fielder (1969) and Rodi (1975), and with respect to swirling jets by Chigier & Chervinsky (1967), Pratte & Keffer (1972) and Ogawa, Hatakeyama & Fujita (1981, 1982). On the basis of the available experimental data it has, however, been found that the self-preservation of a

turbulent, free swirling jet occurs as an asymptotic state, which may only be achieved at a distance sufficiently far from the nozzle. That is why a more general approach to the problem in question seems to result from the semi-preservation hypothesis, as suggested by Elsner & Drobniak (1979). According to this conception, the transverse distribution of each mean as well as each turbulent quantity may be described by using its own length (l^*) and velocity (U^*) scales in terms of properly chosen non-dimensional functions F of relative coordinates $\eta = r/l^*$.

The purpose of this work is to formulate the conditions of the semi-preserving development of a non-isothermal free swirling jet and to analyse the possibilities of its transition into the self-preservation state.

2. Theoretical considerations

The theoretical description of a steady, non-isothermal free swirling jet may be considerably simplified by the assumption that the amount of heat supplied to the fluid is too small to affect the dynamics of the flow. Under such circumstances it seems reasonable to assume that the variation of fluid density, especially in the fully developed flow region, may be disregarded. By taking advantage of the boundary-layer approximations and neglecting the molecular terms, which are small when compared with the turbulent ones, the transport equations of mass, momentum and heat may, respectively, be written as follows:

$$\frac{\partial(r\bar{U}_x)}{\partial x}+\frac{\partial(r\bar{U}_r)}{\partial r}=0, \tag{1}$$

$$\bar{U}_x\frac{\partial\bar{U}_x}{\partial x}+\bar{U}_r\frac{\partial\bar{U}_x}{\partial r}=\boxed{-\frac{1}{\rho}\frac{\partial\bar{p}}{\partial x}-\frac{\partial\overline{u_x^2}}{\partial x}}-\frac{1}{r}\frac{\partial}{\partial r}(r\,\overline{u_x u_r}), \tag{2}$$

$$\frac{1}{\rho}\frac{\partial\bar{p}}{\partial r}=\frac{\bar{U}_\varphi^2}{r}\boxed{+\frac{\overline{u_\varphi^2}}{r}-\frac{1}{r}\frac{\partial}{\partial r}(r\,\overline{u_r^2})}, \tag{3}$$

$$\bar{U}_x\frac{\partial\bar{U}_\varphi}{\partial x}+\bar{U}_r\frac{\partial\bar{U}_\varphi}{\partial r}+\frac{\bar{U}_r\bar{U}_\varphi}{r}=-\frac{1}{r^2}\frac{\partial}{\partial r}(r^2\,\overline{u_r u_\varphi}), \tag{4}$$

$$\bar{U}_x\frac{\partial\bar{\Theta}}{\partial x}+\bar{U}_r\frac{\partial\bar{\Theta}}{\partial r}=-\frac{1}{r}\frac{\partial}{\partial r}(r\,\overline{u_r\vartheta}). \tag{5}$$

From the above equations, after applying the appropriate boundary conditions corresponding to a free jet issuing into a quiescent environment and neglecting the higher-order terms, one may derive the additional integral relations:

$$\frac{\mathrm{d}}{\mathrm{d}x}\int_0^\infty(\bar{U}_x^2-0.5\,\bar{U}_\varphi^2)\,r\,\mathrm{d}r=0, \tag{6}$$

$$\frac{\mathrm{d}}{\mathrm{d}x}\int_0^\infty\bar{U}_x\bar{U}_\varphi r^2\,\mathrm{d}r=0, \tag{7}$$

$$\frac{\mathrm{d}}{\mathrm{d}x}\int_0^\infty\bar{\Theta}\,\bar{U}_x\,r\,\mathrm{d}r=0, \tag{8}$$

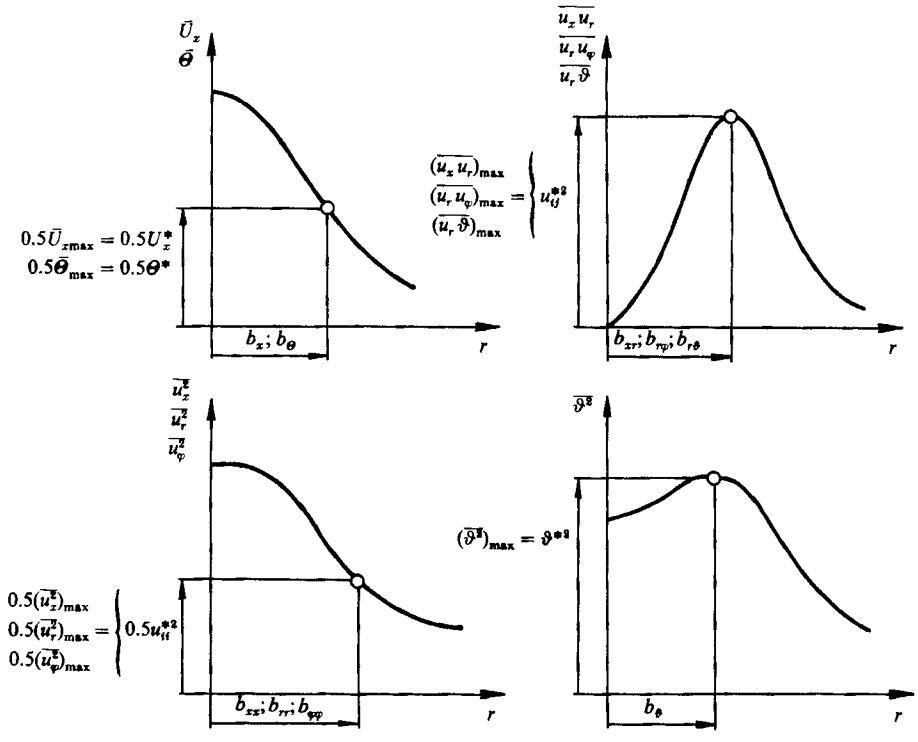

FIGURE 1. Characteristic scales of mean and turbulent quantities.

which express the conversation laws of the axial fluxes of axial and angular momenta and heat, respectively.

It is worth noting that, according to the experimental evidence, the tangential mean velocity component $\bar{U}_\varphi$ decays at a considerably faster rate than the axial mean velocity $\bar{U}_x$. Thus, at a certain distance downstream from the nozzle, (6) may be rewritten in a simplified form

$$\frac{\mathrm{d}}{\mathrm{d}x}\int_0^\infty \bar{U}_x^2 r\,\mathrm{d}r = 0. \tag{9}$$

It should be emphasized that the simplifications that lead to the above relations are valid, at most, at a moderate turbulence level only and cannot be applied to a near flow region of a strongly swirled jet, where intense mixing processes occur.

Now, let us assume that, according to the concept of semi-preservation, all the mean ($\bar{A}_i$) and turbulent ($\overline{\alpha_i \beta_j}$) quantities can be written in the general form

$$\left.\begin{aligned} \bar{A}_i(x,r) &= A_i^*(x) F_i(r/b_i) \\ \overline{\alpha_i \beta_j}(x,r) &= a_{ij}^{*2} F_{ij}(r/b_{ij}) \end{aligned}\right\} \quad i,j = x,r,\varphi,p,\Theta,\vartheta \tag{10}$$

by means of a different velocity or temperature scale (A_i^*, a_{ij}^*) and a different lengthscale (b_i, b_{ij}) for each variable.

The meaning of the particular scales, being functions of x alone, is explained in figure 1. It is reasonable to assume that in a semi-preserving region of a swirling jet all the length-scales are mutually proportional, e.g.

$$\frac{b_{xx}(x)}{b_x(x)} = \text{const}; \quad \frac{b_{r\vartheta}}{b_x(x)} = \text{const}; \ldots, \tag{11}$$

and may therefore be replaced by one arbitrarily chosen scale, for example mean velocity half-width $b_x \equiv b$, which allows all the non-dimensional functions F to be expressed in terms of only one relative coordinate $\eta = r/b(x)$.

The semi-preserving region of a swirling jet may only be achieved at a distance sufficiently far from the nozzle, where the terms in boxes in (2) and (3) may be disregarded as negligibly small. Taking advantage of this assumption and substituting (10) with $b_{ij} \equiv b$ into (1)–(5), (7)–(9) we obtain

$$
\left.
\begin{aligned}
&F_x \frac{\mathrm{d}U_x^*}{\mathrm{d}x} - \eta F'_x \frac{U_x^*}{b}\frac{\mathrm{d}b}{\mathrm{d}x} + \left(F'_r + \frac{F_r}{\eta}\right)\frac{U_r^*}{b} = 0;\\
&U_x^* \frac{\mathrm{d}U_x^*}{\mathrm{d}x} F_x^2 - \frac{U_x^{*2}}{b}\frac{\mathrm{d}b}{\mathrm{d}x}\eta F'_x F_x + \frac{U_r^* U_x^*}{b} F_r F'_x = -\frac{u_{xr}^{*2}}{b}\left(F'_{xr} + \frac{F_{xr}}{\eta}\right);\\
&\frac{U_\varphi^{*2}}{b}\frac{F_\varphi^2}{\eta} = -\frac{p^*}{b}\frac{F'_\mathrm{p}}{\rho};\\
&U_x^* \frac{\mathrm{d}U_\varphi^*}{\mathrm{d}x} F_x F_\varphi - U_x^* \frac{U_\varphi^*}{b}\frac{\mathrm{d}b}{\mathrm{d}x} F'_\varphi F_x \eta + U_r^* \frac{U_\varphi^*}{b}\left(F_r F'_\varphi + \frac{F_r F_\varphi}{\eta}\right) = -\frac{u_{r\varphi}^{*2}}{b}\left(F'_{r\varphi} + 2\frac{F_{r\varphi}}{\eta}\right);\\
&U_x^* \frac{\mathrm{d}\Theta^*}{\mathrm{d}x} F_x F_\Theta - U_x^* \frac{\Theta^*}{b}\frac{\mathrm{d}b}{\mathrm{d}x} F_x F'_\Theta \eta + U_r^* \frac{\Theta^*}{b} F_r F'_\Theta = -\frac{u_{r\vartheta}^{*2}}{b}\left(F'_{r\vartheta} + \frac{F_{r\vartheta}}{\eta}\right);\\
&\frac{\mathrm{d}}{\mathrm{d}x}\int_0^\infty U_x^{*2} b^2 F_x^2 \eta \,\mathrm{d}\eta = 0;\\
&\frac{\mathrm{d}}{\mathrm{d}x}\int_0^\infty U_x^* U_\varphi^* F_x F_\varphi b^3 \eta^2 \,\mathrm{d}\eta = 0;\\
&\frac{\mathrm{d}}{\mathrm{d}x}\int_0^\infty U_x^* \Theta^* b^2 F_x F_\Theta \eta \,\mathrm{d}\eta = 0;
\end{aligned}
\right\} \tag{12}
$$

where F' denotes differentiation with respect to η.

If the flow is semi-preserving, the above set of equations relates the universal functions F and must be identical in meaning for all values of x and η. This requires that the coefficients of the various terms in each equation be mutually proportional. The condition of semi-preserving development makes it possible to express all the velocity, temperature and pressure scales as functions of the lengthscale b alone, according to relationships

$$
\left.
\begin{aligned}
&U_x^* \sim \frac{1}{b}; \qquad U_r^* \sim \frac{1}{b}\frac{\mathrm{d}b}{\mathrm{d}x}; \qquad U_\varphi^* \sim \frac{1}{b^2};\\
&\Theta^* \sim \frac{1}{b}; \qquad u_{xr}^{*2} \sim \frac{1}{b^2}\frac{\mathrm{d}b}{\mathrm{d}x}; \qquad u_{r\varphi}^{*2} \sim \frac{1}{b^3}\frac{\mathrm{d}b}{\mathrm{d}x};\\
&u_{\vartheta\varphi}^{*2} \sim \frac{1}{b^2}\frac{\mathrm{d}b}{\mathrm{d}x}; \qquad p^* \sim \frac{1}{b^4}.
\end{aligned}
\right\} \tag{13}
$$

In Elsner & Kurzak (1987) it was pointed out that, starting at a distance $x \simeq 8D$ from the nozzle, the mean velocity and mean temperature profiles plotted in non-dimensional forms $\bar{U}/\bar{U}_{\max}$ and $\bar{\Theta}/\bar{\Theta}_{\max}$ in terms of a relative coordinate $\eta = r/b$ show a certain similarity. At approximately the same distance, the lateral extent of the

non-isothermal free swirling jet, determined both by the mean velocity half-width b and by the mean temperature half-width b_Θ, increases linearly with x, according to the relationships

$$\left.\begin{aligned} \frac{b}{D} &= B(s)\frac{x-x_0(s)}{D}, \\ \frac{b_\Theta}{D} &= B_\Theta(s)\frac{x-x_0(s)}{D}, \end{aligned}\right\} \tag{14}$$

where D is the nozzle outlet diameter and x_0 denotes the localization of the so-called virtual origin of flow, being dependent on the swirl degree, as follows:

$$\frac{x_0}{D} = -3.5s. \tag{15}$$

The swirl degree

$$s = \frac{\int_0^\infty \rho \bar{U}_x \bar{U}_\varphi r^2 \,\mathrm{d}r}{R\int_0^\infty \rho(\bar{U}_x^2 - 0.5\,\bar{U}_\varphi^2) r \,\mathrm{d}r} \tag{16}$$

is defined here as the axial flux of swirl momentum divided by the axial flux of axial momentum times nozzle radius R.

It is reasonable to suppose that at a certain distance from the nozzle outlet the other lengthscales characterizing, according to figure 1, the distributions of turbulent quantities may also become linear functions of the x-coordinate, thus confirming the validity of the assumption

$$b_{xr} \sim b_{r\varphi} \sim b_{r\vartheta} \sim \ldots \sim b_x \equiv b. \tag{17}$$

By introducing the conditions

$$b \sim (x-x_0); \quad \frac{\mathrm{d}b}{\mathrm{d}x} = \text{const}$$

into (13), we finally get

$$\left.\begin{aligned} &\bar{U}_x \sim \bar{U}_r \sim \bar{\Theta} \sim (x-x_0)^{-1}, \\ &\bar{U}_\varphi \sim \overline{u_x u_r} \sim \overline{u_r \vartheta} \sim (x-x_0)^{-2}, \\ &\overline{u_r u_\varphi} \sim (x-x_0)^{-3}; \quad p_\infty - \bar{p} \sim (x-x_0)^{-4}. \end{aligned}\right\} \tag{18}$$

Relations (18) characterizing the law of semi-preserving development of non-isothermal free swirling jets are usually completed by the expression

$$\overline{u_x^2} \sim \overline{u_r^2} \sim \overline{u_\varphi^2} \sim (x-x_0)^{-2} \tag{19}$$

which results from the neglected terms of the transport equations.

In order to achieve a more thorough insight into the turbulence structure we can analyse the behaviour of correlation coefficients R_{xr} and $R_{r\varphi}$, which determine the statistical connection between the appropriate terms of the Reynolds stress tensor. Considering (18) and (19) we have

$$\left.\begin{aligned} R_{xr} &= \frac{\overline{u_x u_r}}{(\overline{u_x^2})^{\frac{1}{2}}(\overline{u_r^2})^{\frac{1}{2}}} \sim x^0 = \text{const}, \\ R_{r\varphi} &= \frac{\overline{u_r u_\varphi}}{(\overline{u_r^2})^{\frac{1}{2}}(\overline{u_\varphi^2})^{\frac{1}{2}}} \sim x^{-1}. \end{aligned}\right\} \tag{20}$$

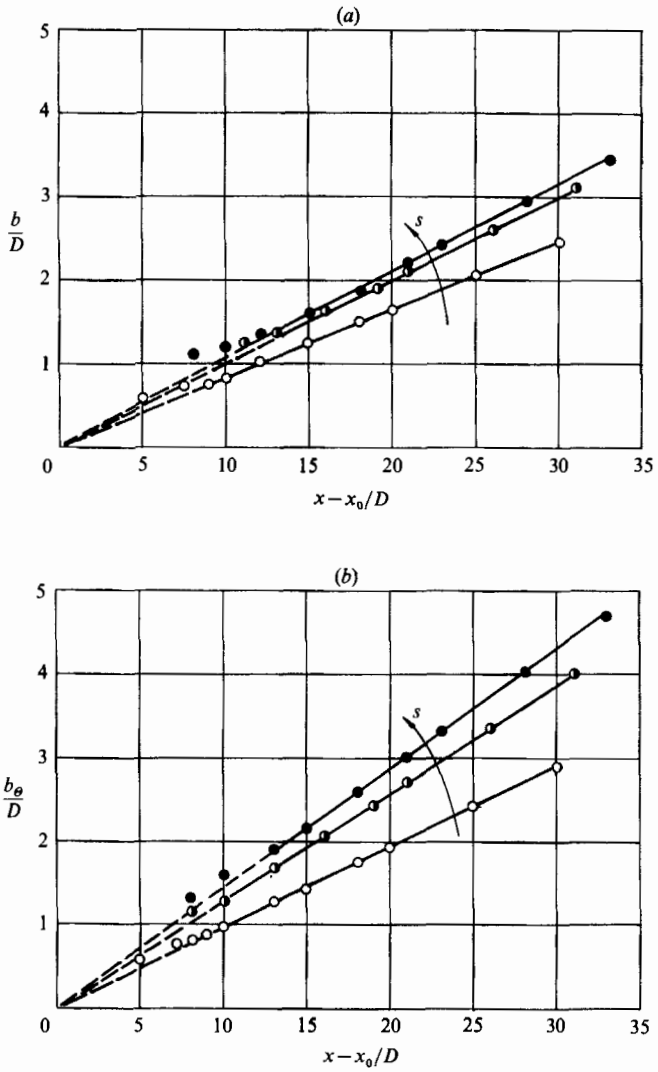

FIGURE 2. Streamwise variations of the lengthscales characterizing the distributions of (*a*) mean velocity component $\bar{U}_x$ (*b*) mean temperature $\bar{\Theta}$ at $\bar{\Theta}_{axe} = 40$ °C (○, $s = 0$; ◑, 0.31; ●, 0.42).

The above formulae clearly show that these terms of the turbulence stress tensor do not maintain mutual proportionality during decay. Such proportionality, which is the basic condition of self-preservation, may only be achieved at a distance where the shear stress $\overline{u_r u_\varphi}$ becomes negligible compared with the value of $\overline{u_x u_r}$ because of its faster decrease. Thus, we can see that self-preservation is in fact an asymptotic state or a final stage of the semi-preserving development, which can be achieved when the swirling jet turns into an unswirled flow.

3. Experimental procedure

In order to check the validity of the semi-preservation concept outlined in the previous section a series of experimental investigations was performed in a low-speed, open-circuit wind tunnel with a circular outlet nozzle 40 mm in diameter. The

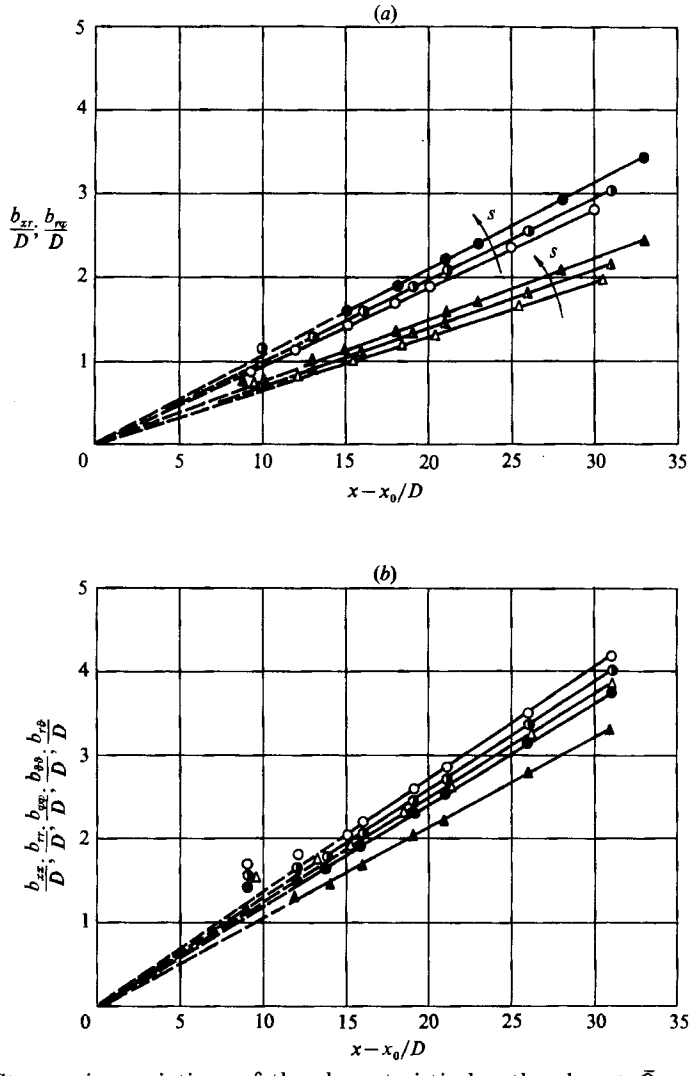

FIGURE 3. Streamwise variations of the characteristic lengthscales at $\bar{\Theta}_{ave} = 40$ °C. (*a*) b_{xr}: ○, $s = 0$; ◑, 0.31; ●, 0.42; and $b_{r\varphi}$: △, $s = 0.22$; ◭, 0.31; ▲, 0.42, (*b*) ○, b_{xx}; ◑, b_{rr}; ●, $b_{\varphi\varphi}$; △, $b_{\vartheta\vartheta}$; ▲, $b_{r\vartheta}$, for $s = 0.31$.

swirl was produced by means of exchangeable sets of angled vanes, making it possible to obtain different values of swirl degree within the range $s \leqslant 0.42$.

For all the swirl degrees the flow rate was maintained at a constant level, corresponding to the Reynolds number $Re_D \approx 8 \times 10^4$ based on the axial velocity $\bar{U}_{ave} \approx 37$ m/s averaged at the nozzle exit. The air flowing through the wind tunnel was heated electrically to a temperature $\bar{\Theta}_{ave} = 40$ °C, above the ambient one. This value was kept constant during experiment by controlling the heat flux delivered to the fluid.

Turbulence characteristics and mean temperature were measured using a 3-channel DISA 55 M System hot-wire anemometer, while the mean-velocity field was determined by means of a miniature five-hold spherical probe. The full description of the test apparatus and experimental procedure applied was given by Elsner &

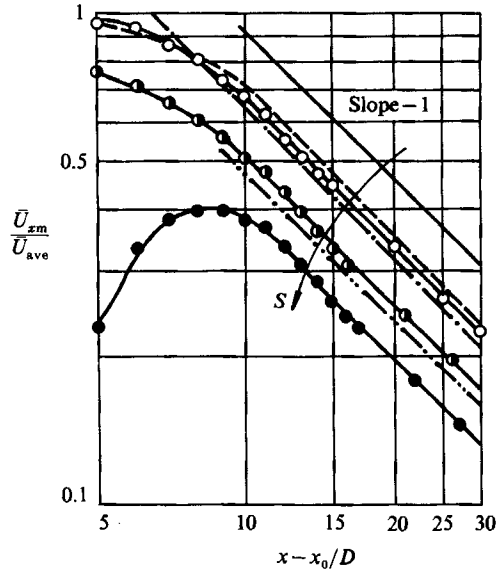

FIGURE 4. Downstream evolution of $\bar{U}_{xm}/\bar{U}_{ave}$ at $\bar{\Theta}_{ave} = 40$ °C: ○, $s = 0$; ◑, 0.31; ●, 0.42; ——, after Komori & Ueda (1984) for $s = 0$; –·–·–·, –··–··–, after Ogawa & Hatakeyama (1979), for $s = 0$ and 0.505, respectively.

Kurzak (1987). However, in comparison with those measurements, the present experiment covered an axial distance that was twice as large, i.e. up to $x = 30D$, in order to analyse the similarity of turbulent quantities that might occur in that region.

4. Experimental results

4.1. *Evolution of the lengthscales*

Figure 2 presents the variation of the axial-mean-velocity half-width b and the mean-temperature half-width b_Θ defined by the relation (see also figure 1)

$$\bar{U}_x(b) = 0.5\bar{U}_{x_{max}}; \quad \bar{\Theta}(b_\Theta) = 0.5\bar{\Theta}_{max}.$$

As may be seen, starting at $x-x_0 \approx (8-12)\,D$, both these scales appear to be linear functions of the x-coordinate, in accordance with (14).

The lengthscales b_{xr} and $b_{r\varphi}$, characterizing the distributions of turbulent shear stresses $\overline{u_x u_r}$ and $\overline{u_r u_\varphi}$, are shown in figure 3(*a*) for three swirl degrees. As may be seen, at the distance $x-x_0 \gtrsim 15\,D$ both the scales appear to be linear function of the coordinate $x-x_0$, independent of the swirl degree. However, the slopes of the lines presented on this graph tend to increase with the growth of swirl as a consequence of the more intense radial spread of the jet under the swirl action.

All the remaining lengthscales are shown in terms of $x-x_0$ in figure 3(*b*), but this time for only one intermediate value of s. The curves presented there tend to straighten with downstream distance. This confirms the assumption that in the sufficiently far flow region all the lengthscales become mutually proportional and may therefore be expressed in terms of one arbitrarily chosen scale, e.g. axial-mean-velocity half-width b. It is worth noting here that the linear character of the lengthscales related to the turbulent quantities is established at a distance

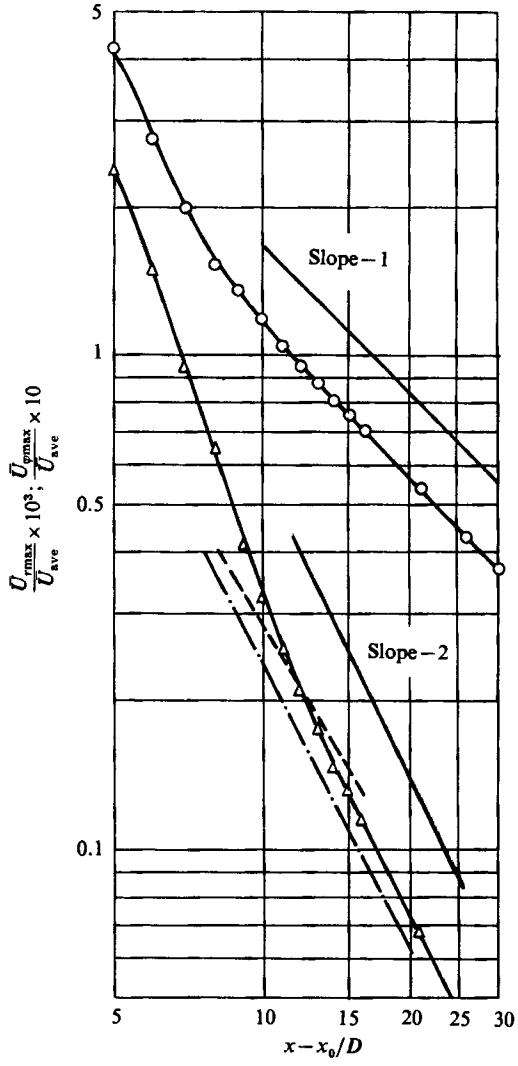

FIGURE 5. Downstream evolution of mean velocity components at $\bar{\Theta}_{ave} = 40$ °C and $s = 0.31$: ○, U_{rmax}/U_{ave}; △, $U_{\varphi max}/U_{ave}$; ---, after Chigier & Chervinsky (1967) for $s = (0.234–0.640)$; -·-·-, after Ogawa & Hatakeyama (1981) for $s = 0.505$.

considerably farther from the nozzle than that of the scale that correspond to the mean velocithy and temperature fields. This reflects the overall tendency of the turbulence structure to attain similarity farther downstream than the mean-flow pattern.

4.2. *Variation of the mean-flow scales*

The evolution of the axial mean velocity component U_{xm}, measured at the jet axis, is shown in figure 4 for three different swirl degrees. Starting approximately at the distance $x - x_0 \approx (12–15)\,D$ the curves plotted in log–log coordinates become parallel straight lines of slope -1, which verifies the theoretical prediction given by (18). An increase in swirl degree is accompanied by a simultaneous decrease in the U_{xm} value, caused by the faster radial spread of the jet under the swirl action. For comparison, figure 4 also shows the results obtained by Ogawa & Hatakeyama (1979) as well as

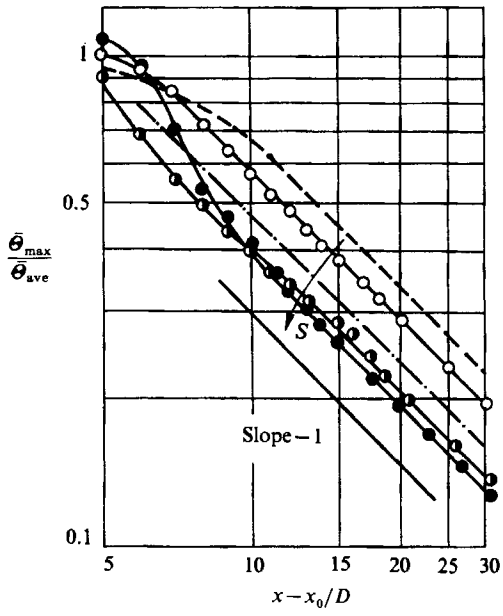

FIGURE 6. Downstream evolution of mean temperatures $\bar{\Theta}_m/\bar{\Theta}_{ave}$ at $\bar{\Theta}_{ave} = 40$ °C for various swirl degrees: ○, $s = 0$; ◑, 0.31; ●, 0.42; – – –, after Komori & Ueda (1984) for $s = 0.2$, $\bar{\Theta}_{ave} = 20$ °C; –·–·–, after Ogawa & Hatakeyama (1981) for $s = 0$.

by Komori & Ueda (1984). As may be seen, their findings agree fairly well with the experimental data of the present study.

The variations of the maximum values of the remaining mean velocity components $\bar{U}_r$ and $\bar{U}_\varphi$ are shown in figure 5 for an intermediate swirl degree $s = 0.31$. For comparison, results for the $\bar{U}_\varphi$ decay are included, taken from Chigier & Chervinsky (1967) and Ogawa & Hatakeyama (1981). As may be seen, in accordance with theoretical predictions, the curves presented may be respectively described by the power functions

$$\bar{U}_r \sim (x-x_0)^{-1}; \quad \bar{U}_\varphi \sim (x-x_0)^{-2}.$$

The evolution of the maximum mean temperature $\bar{\Theta}$ is illustrated in figure 6 and compared with the available data of Komori & Ueda (1984) and Ogawa & Hatakeyama (1981) for $s = 0$. The results obtained also show the following dependence on the streamwise coordinate:

$$\bar{\Theta}_{max} \sim (x-x_0)^{-1}.$$

4.3. *Downstream decay of the turbulent quantities*

As the swirl causes a more intense radial spread of the jet it seems reasonable to expect that its growth should be accompanied by a decrease in the majority of flow quantities. However, such a rule does not include the quantities directly connected with the tangential motion of fluid. This is clearly demonstrated in figure 7 where the downstream evolution of the maximum value of turbulent shear stresses $\overline{u_x u_r}$ and $\overline{u_r u_\varphi}$ is shown in a normalized form for three different swirl degrees. As can be seen, the swirl exerts an opposing effect on each of these shear stresses, decreasing the $\overline{u_x u_r}$ values and increasing the $\overline{u_r u_\varphi}$ stress. Beyond $x-x_0 > (15\text{–}20)\,D$ the curves plotted in log–log coordinates become straight lines, with slopes -2 and -3,

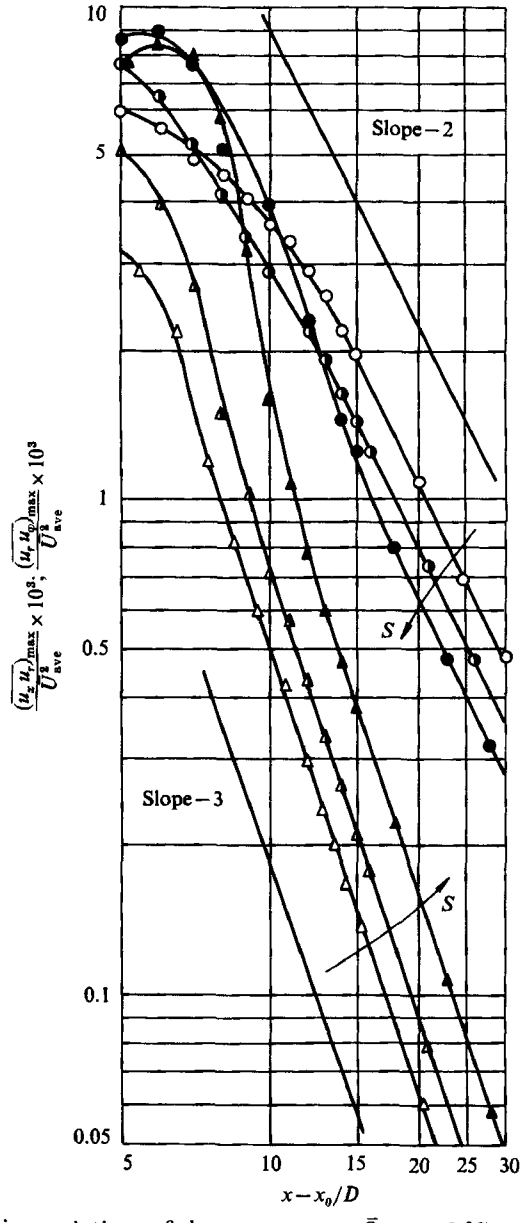

FIGURE 7. Streamwise variations of shear stresses at $\bar{\Theta}_{ave} = 40$ °C. $(\overline{u_x u_r})_{max}/\bar{U}^2_{ave}$: ○, $s = 0$; ◑, 0.31; ●, 0.42; and $(\overline{u_r u_\varphi})_{max}/\bar{U}^2_{ave}$: △, $s = 0.22$; ◭, 0.31; ▲, 0.42.

respectively. This verifies the theoretical prediction that the decay of the turbulent shear stresses follows the power-law dependence

$$\overline{u_x u_r} \sim (x-x_o)^{-2}; \quad \overline{u_r u_\varphi} \sim (x-x_0)^{-3}.$$

The downstream evolution of the maximum values of the normal turbulent stresses, normalized by $\bar{U}^2_{ave}$ and plotted for one swirl degree in a log–log system in figure 8, shows that, starting at $x-x_0 \approx 20\,D$, all are power functions of $x-x_0$:

$$\overline{u_x^2} \sim \overline{u_r^2} \sim \overline{u_\varphi^2} \sim (x-x_0)^{-2}.$$

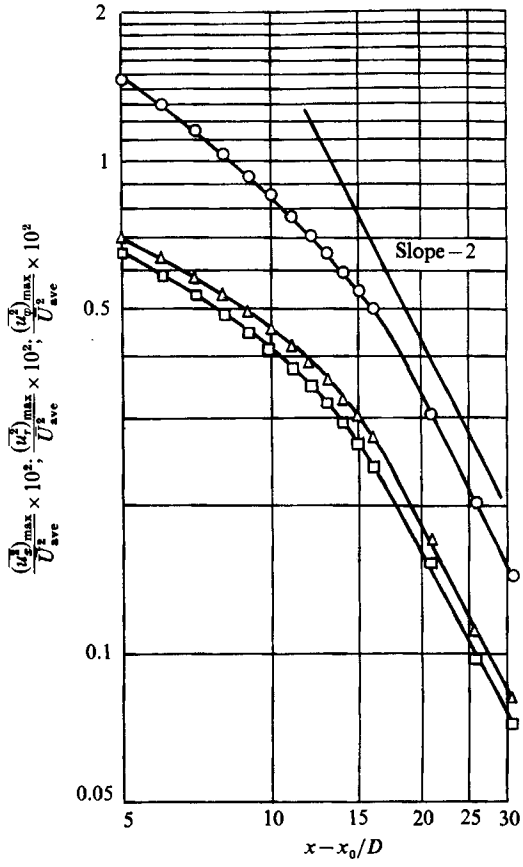

FIGURE 8. Streamwise variations of normal stresses at $\Theta_{ave} = 40$ °C for $s = 0.31$: ○, $(\overline{u_x^2})_{max}/\bar{U}^2_{ave}$; △, $(\overline{u_r^2})_{max}/\bar{U}^2_{ave}$; □, $\overline{u^2_{\varphi max}}/\bar{U}^2_{ave}$.

Moreover, the streamwise component is always larger than the lateral ones and reaches a ratio of almost two to one.

The maximum values of temperature variance $\overline{\vartheta^2}$ and turbulent heat flux $\overline{u_r \vartheta}$ presented for three swirl degrees in figure 9 also show, at $x-x_0 > 15\,D$, the power-law dependence on streamwise coordinate

$$\overline{\vartheta^2} \sim \overline{u_r \vartheta} \sim (x-x_0)^{-2},$$

thus confirming the semi-preserving condition described by (18).

4.4. *Radial distributions of turbulent quantities*

It is generally believed, supported by the measurements of Chigier & Chervinsky (1967), Ogawa & Hatakeyama (1981), Elsner & Kurzak (1987) and others, that the radial distributions of mean-flow quantities in free, swirling jets become reasonably similar some few diameters downstream of the nozzle, for example at $x/D \approx 8$. However, it might be expected that the turbulent quantities would achieve their universal profiles more slowly, at a considerably later stage of decay. This is confirmed by the examples of distributions of the normal turbulent stress $\overline{u_x^2}$ presented in normalized form in figure 10 and compared with the results of Pratte & Keffer (1972). As may be seen, the data points do not begin to group sufficiently well

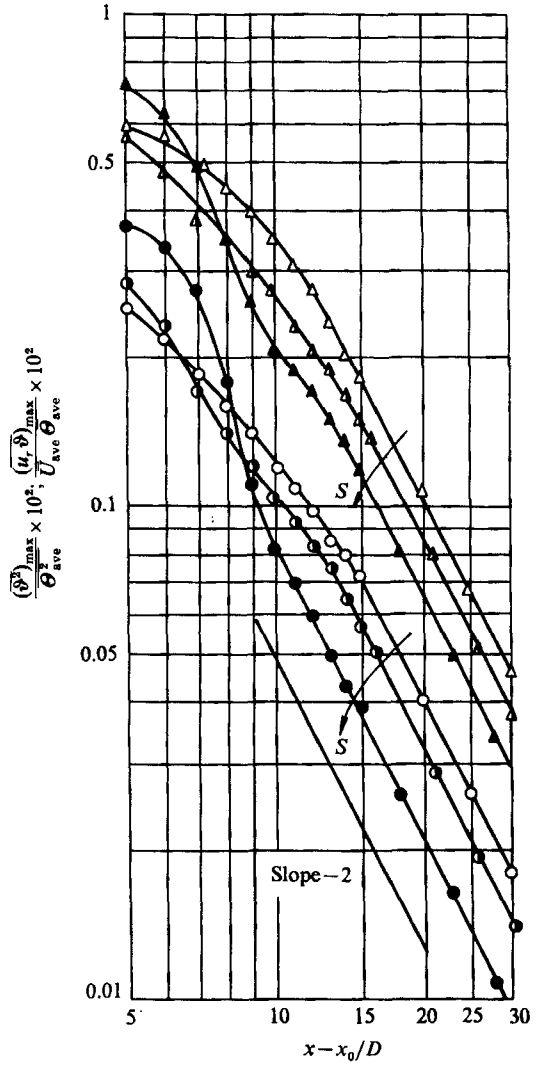

FIGURE 9. Streamwise variations of $(\overline{\vartheta^2})_{max}/\bar{\Theta}^2_{ave}$: △, $s = 0$; ◭, 0.31; ▲, 0.42; and $(\overline{u_r\vartheta})_{max}/\bar{U}_{ave}\bar{\Theta}_{ave}$: ○, $s = 0$; ◑, 0.31; ●, 0.42 at $\bar{\Theta}_{ave} = 40$ °C.

about the common curve until $x/D = 12$, namely, much further than in the case of mean quantities, which have a universal form at $x/D \approx 8$.

Radial distributions of turbulent shear stresses $\overline{u_x u_r}$, $\overline{u_r u_\varphi}$ and turbulent heat flux $\overline{u_r \vartheta}$, normalized by their maximum values, are shown in figures 11, 12 and 13, respectively. The available data of Pratte & Keffer (1972) and Komori & Ueda (1984), also plotted for comparison, show, however, some disagreement with the present results, especially in the outer part of the jet. Although $\overline{u_x u_r}$ and $\overline{u_r \vartheta}$ are very similar to each other and reach their maxima at practically the same point determined by the coordinate $\eta \approx 0.8$, the profile of shear stress $\overline{u_r u_\varphi}$ exhibits a somewhat different form and has its maximum shifted towards the jet axis, at $\eta \approx 0.6$.

Normalized distributions of the mean-square value of temperature fluctuations,

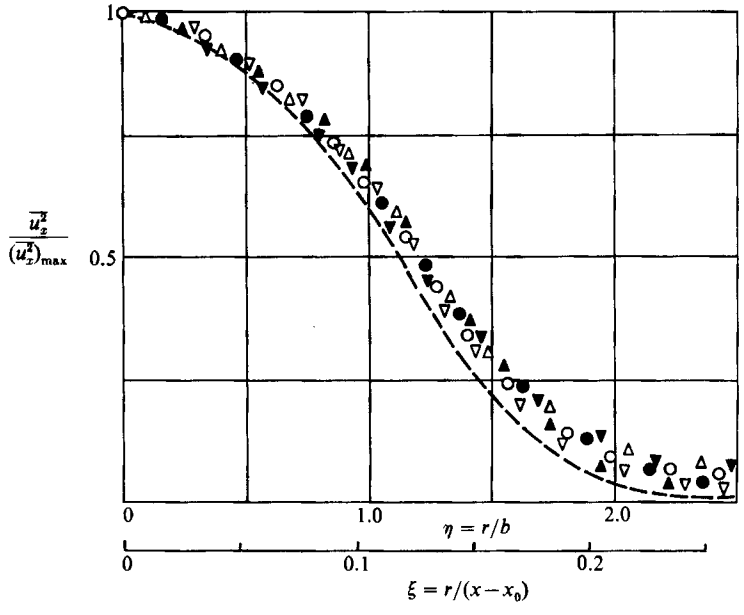

FIGURE 10. Normalized radial distributions of $\overline{u_x^2}$ at $\bar{\Theta}_{ave} = 40$ °C and $s = 0.31$ for various axial distances: ○, $x/D = 12$; ●, 15; △, 18; ▲, 20; ▽, 25; ▼, 30; ---, after Pratte & Keffer (1972) for $s = 0.3$, $x/D = 12$ and 30.

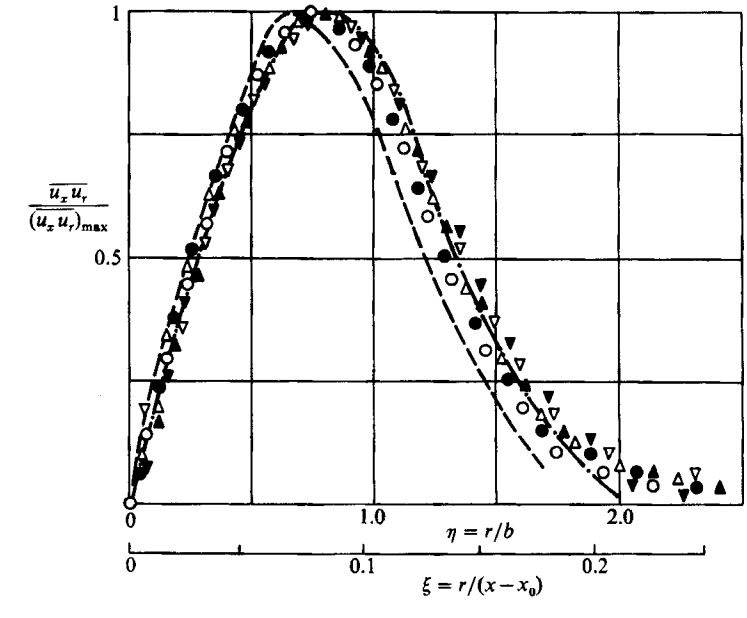

FIGURE 11. Normalized radial distributions of $\overline{u_x u_r}$ at $\bar{\Theta}_{ave} = 40$ °C and $s = 0.31$ for various axial distances: ○, $x/D = 12$; ●, 15; △, 18; ▲, 20; ▽, 25; ▼, 30; ——, after Komori & Ueda (1984) for $x/D = 47$, $s = 0$, $\bar{\Theta}_{ave} = 20$ °C; -·-·-·-, after Pratte & Keffer (1972) for $x/D = 12$, $s = 0$, $\bar{\Theta}_{ave} = 0$.

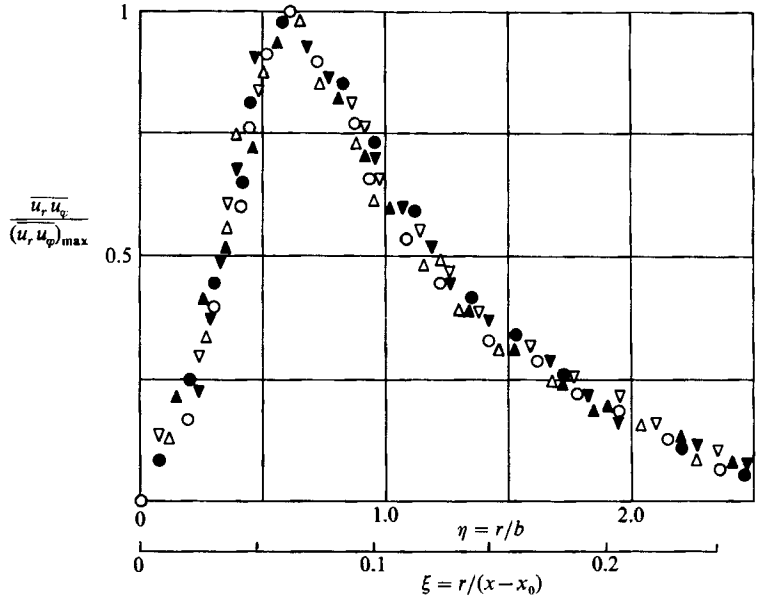

FIGURE 12. Normalized radial distributions of $\overline{u_r u_\varphi}$ at $\bar{\Theta}_{ave} = 40$ °C and $s = 0.31$ for various axial distances: ○, $x/D = 12$; ●, 15; △, 18; ▲, 20; ▽, 25; ▼, 30.

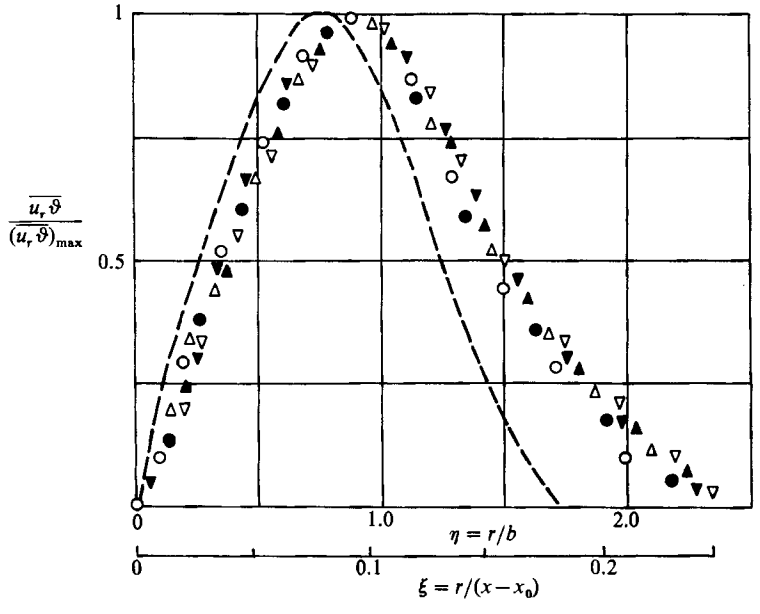

FIGURE 13. Normalized radial distributions of $\overline{u_r \vartheta}$ at $\bar{\Theta}_{ave} = 40$ °C and $s = 0.31$ for various axial distances: ○, $x/D = 12$; ●, 15; △, 18; ▲, 20; ▽, 25; ▼, 30; ---, after Komori & Ueda (1984) for $x/D = 47$, $s = 0$, $\bar{\Theta}_{ave} = 20$ °C.

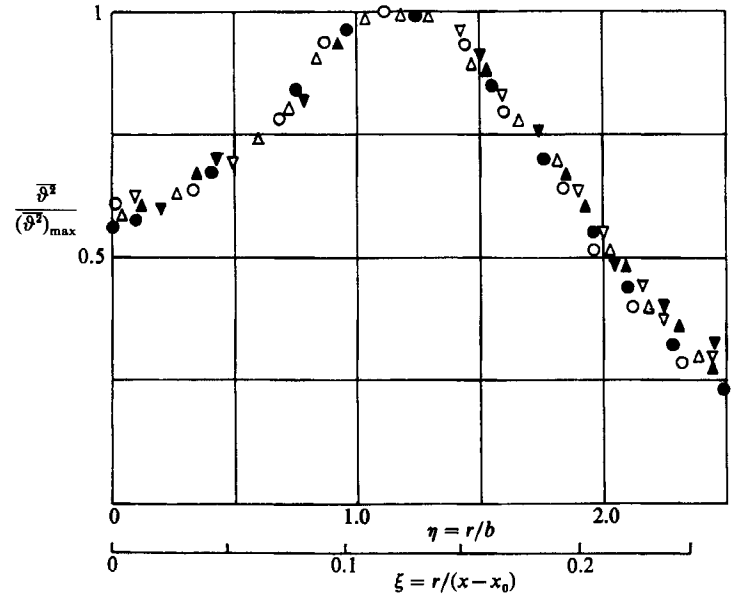

FIGURE 14. Normalized radial distributions of $\overline{\vartheta^2}$ at $\bar{\Theta}_{ave} = 40$ °C and $s = 0.31$ for various axial distances: ○, $x/D = 12$; ●, 15; △, 18; ▲, 20; ▽, 25; ▼, 30.

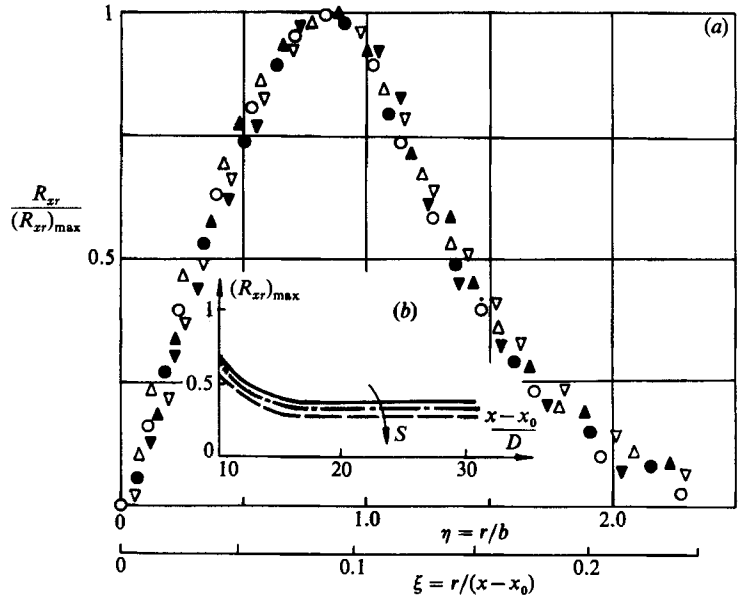

FIGURE 15. Correlation coefficient R_{xr} at $\bar{\Theta}_{ave} = 40$ °C. (*a*) Normalized radial distribution at $s = 0.31$ for various axial distances: ○, $x/D = 12$; ●, 15; △, 18; ▲, 20; ▽, 25; ▼, 30. (*b*) Streamwise evolution for various swirl degrees: ——, $s = 0$; –·–·, 0.31; – – –, 0.42.

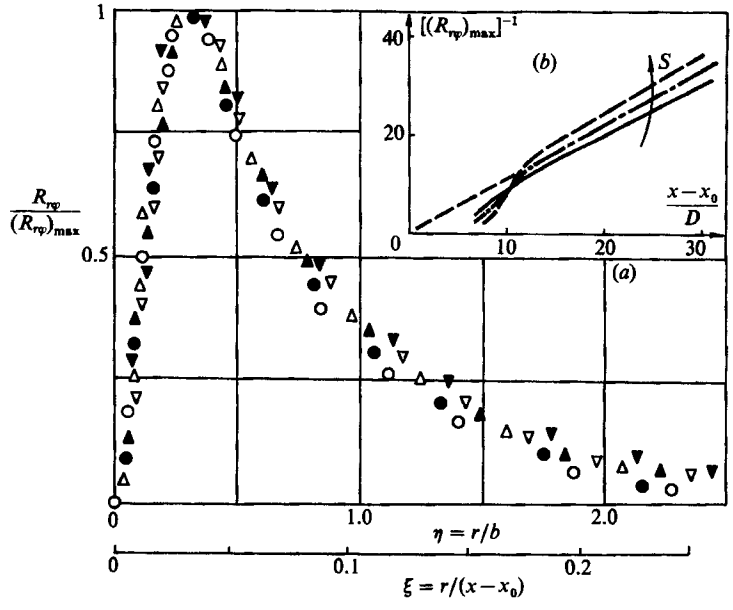

FIGURE 16. Correlation coefficient $R_{r\varphi}$ at $\bar{\Theta}_{ave} = 40$ °C. (*a*) Normalized radial distribution at $s = 0.31$ for various axial distances: ○, $x/D = 12$; ●, 15; △, 18; ▲, 20; ▽, 25; ▼, 30. (*b*) Streamwise evolution for various swirl degrees: ——, $s = 0.22$; –·–·, 0.31; – – –, 0.42.

plotted in figure 14, also appear to stabilize their universal form at a distance $x-x_0 > 12\,D$, and confirm the previous observations of Komori & Ueda (1984) and Elsner & Kurzak (1987) that the radial extent of the temperature field is greater than the radial extent of the velocity field.

4.5. *The behaviour of correlation coefficients*

According to the definition given by Stewart & Townsend (1951) the basic requirement of self-preservation is to maintain a similarity of turbulent structure during decay. It means that all the components of the turbulent stress tensor should be mutually proportional along any arbitrarily chosen streamline. In particular such a demand requires constant values of the correlations R_{xr} and $R_{r\varphi}$, and this may be examined on the basis of the data presented in figures 15 and 16.

As may be seen, although the radial distributions of both these correlation coefficients, when normalized, group fairly well about the common curves, the downstream evolution of their maximum values shows significant differences. The coefficient $(R_{xr})_{max}$ (figure 15*b*), in accordance with the theoretical predictions given by (20), stabilizes, starting at $x-x_0 \approx 20\,D$, at an almost constant level, depending on the swirl degree. However, such a tendency cannot be observed for $(R_{r\varphi})_{max}$ which, as shown in figure 16(*b*), decreases continuously in the downstream direction and starting at $x-x_0 \approx (15\text{–}17)\,D$ appears to be inversely proportional to the streamwise coordinate:

$$R_{r\varphi} \sim (x-x_0)^{-1}.$$

It is worth noting that the correlation coefficient $< \mathrm{R}_{r\theta}$ (figure 17) describing the statistical relationship between velocity and temperature fluctuations shows a close resemblance to the R_{xr} behaviour and at $x-x_0 \approx 15\,D$ its maximum value reaches a constant level, dependent only on the swirl degree.

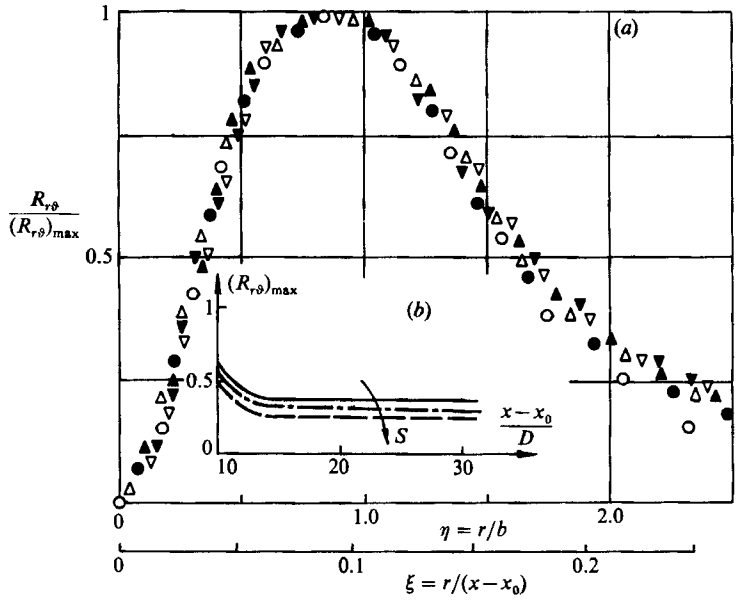

FIGURE 17. Correlation coefficient $R_{r\vartheta}$ at $\bar{\Theta}_{ave} = 40$ °C. (*a*) Normalized radial distribution at $s = 0.31$ for various axial distances: ○, $x/D = 12$; ●, 15; △, 18; ▲, 20; ▽, 25; ▼, 30. (*b*) Streamwise evolution for various swirl degrees: ——, $s = 0$; –·–·, 0.31; – – –, 0.42.

5. Final remarks

The analysis of the experimental data presented above verifies the concept of semi-preservation in a free, non-isothermal swirling jet. It is shown that, in accordance with the theoretical predictions, at a distance sufficiently far from the nozzle, say $x > 12\,D$, the radial distributions of mean and turbulent quantities have universal profiles described by the non-dimensional functions $F(\eta)$. At the same time, starting approximately at the same axial distance, all characteristic length, velocity and temperature scales exhibit a power-law dependence on streamwise coordinate in accordance with (18).

The empirical results obtained in the present study enable one to draw the conclusion that strict self-preservation, which, in particular, calls for the constant value of all the correlation coefficients, may be theoretically achieved as an asymptotic state at a distance infinitely far from the nozzle where each swirling jet transforms into an unswirled one. In practice such a state may be expected at a certain finite distance where the $\overline{u_r u_\varphi}$ stress, owing to its faster decay, becomes at least one order-of-magnitude smaller than the $\overline{u_x u_r}$ stress. As results from the data presented in figure 7 show, the distance at which $\overline{u_r u_\varphi}/\overline{u_x u_r} < 0.1$ depends on the swirl degree and for $s = 0.42$ is $x - x_0 \approx 50\,D$. At the same time, the results plotted in figures 15 and 16 and extrapolated to $x - x_0 \approx 50\,D$, show that at this distance $R_{r\varphi}/R_{xr} \approx 0.05$. It is obvious that the condition $\overline{u_r u_\vartheta}/\overline{u_x u_r} < 0.1$, defining the beginning of the self-preserving region, has a quite arbitrary character. However, it gives some idea as to a possible evaluation of the distance where self-preservation in a swirling jet may be established.

REFERENCES

CHIGIER, N. A. & CHERVINSKY, A. 1967 Experimental investigation of swirling vortex motion in jets. *Trans. ASME* E: *J. Appl. Mech.* **34**, 443.

CURTET, R. M. & DARIGOL, M. 1978 Aerothermique d'un Jet Libre Tournant Turbulent. Preprint, Institute de Mecanique, Grenoble.

ELSNER, J. W. & DROBNIAK, S. 1979 Semi-preserving region in coaxial swirling jets. In *Transportprozesses in turbulenten Strömungen*, Heft I, p. 55. Berlin: Akademie der Wissenschaften der DDR.

ELSNER, J. W. & DROBNIAK, S. 1983 Turbulence structure in swirling jets. In *Structure of Complex Turbulent Shear Flow* (ed. R. Dumas & L. Fulachier), p. 219. Springer.

ELSNER, J. W. & KURZAK, L. 1987 Characteristics of turbulent flow in slightly heated free swirling jets. *J. Fluid. Mech.* **180**, 147.

GRANDMAISON, E. W. & BECKER, H. A. 1982 Turbulent mixing in free swirling jets. *Can. J. Chem. Engng* **60**, 76.

KOMORI, S. & UEDA, H. 1984 Turbulent effects on the chemical reaction for a jet in a nonturbulent stream and for a plume in a grid-generated turbulence. *Phys. Fluids.* **27**, 77.

KOMORI, S. & UEDA, H. 1985 Turblent flow structure in the near field of a swirling round free jet. *Phys. Fluids* **28**, 2075.

OGAWA, A., HATAKEYAMA, H. & FUJITA, H. 1979 Fluiddynamical characteristics of the turbulent straight and rotational jets (1st report). *J. College Engng Nihon Univ.* A **20**, 133.

OGAWA, A., HATAKEYAMA, H. & FUJITA, Y. 1981 Fluiddynamical characteristics of the turbulent straight and rotational jets (2nd report). *J. College Engng Nihon Univ.* A **22**, 157.

OGAWA, A., HATAKEYAMA, H. & FUJITA, Y. 1982 Fluiddynamical characteristics of the turbulent straight and rotational jets (3rd report). *J. College Engng Nihon Univ.* A **23**, 89.

PRATTE, B. D. & KEFFER, J. F. 1972 The swirling turbulent jet. *Trans. ASME* D: *J. Basic Engng* **94**, 739.

RODI, W. A. 1975 A review of experimental data of uniform density free turbulent boundary layers. In *Studies of Convection Theory Measurements and Application* (ed. B. E. Launder), vol. 1, p. 79. Academic.

ROSE, W. R. 1962 A swirling round turbulent jet. 1 Mean-flow measurements. *Trans. ASME* E: *J. Appl. Mech.* **29**, 615.

STEWART, R. W. & TOWNSEND, A. A. 1951 Similarity and self-preservation in isotropic turbulence. *Phil. Trans. R. Soc. Lond.* A **243**, 359.

WYGNANSKI, I. J. & FIEDLER, H. F. 1969 Some measurements in the self-preserving jet. *J. Fluid. Mech.* **38**, 577.